

Compact Half-Unit Imaging Electron Spectrometer for CubeSat Operations (CHICO)

Joshua Méndez
Boston University
8 St Mary's St, Boston, MA 02215
ub313@bu.edu

David Voss
Air Force Research Laboratory
David.Voss@kirtland.af.mil

Francisco Suárez
Boston University
8 St Mary's St, Boston, MA 02215
fjsuarez@bu.edu

Theodore A. Fritz
Boston University, Center for Space Physics
725 Commonwealth Avenue, Boston, MA 02215
fritz@bu.edu

Douglas Carssow
Naval Research Laboratory
dcarssow@space.nrl.navy.mil

Avi Gunda
Boston University
8 St Mary's St, Boston, MA 02215
avigunda@bu.edu

ABSTRACT

Previous satellite missions have demonstrated that portions of the magnetosphere, such as the High Latitude Trapping Boundaries (HLTBs), are very sensitive to solar activity. At the HLTBs, the Earth's field lines combine with the so called Interplanetary Magnetic Field (IMF), and represent the poleward termini of the radiation belts. The relationship of the HLBT to changes in the solar wind and the IMF has not been characterized in any detail and must be studied further. Such exploration will undoubtedly yield insight on how to mitigate the effects of spaceweather phenomena on orbiting spacecraft as well as provide a capability for forecasting.

The Compact Half-unit Imaging electron spectrometer for CubeSat Operations (CHICO) project aims to provide a cost-effective, miniaturized Imaging Electron Spectrometer (IES) to assist in addressing the problem of spaceweather. Designed around the Readout Electronics for Nuclear Applications (RENA3) chip, the instrument will measure energetic particle flux as its host satellite passes through the HLTBs. CHICO occupies a volume smaller than 500 cm³ and is CubeSat-compatible. Despite its minute volume, CHICO is expected to perform similarly to the IES (aka FSH) integrated into the LCI Instrument to be flown on the Air Force Demonstration and Science eXperiments (DSX) mission. We describe the impressive energy and angular resolution for energetic electrons of the CHICO sensor system.

INTRODUCTION

Geophysical Background

The absence of shear waves in the layer between the Earth's lower mantle and the inner core suggests that the outer core is composed of a ferric fluid. It is believed that currents in this highly conductive liquid have given rise to the planet's dipole magnetic field^[1].

Magnetic field lines come in two flavors: open field lines and closed field lines. Closed field lines exit the surface of the planet equatorward of the southern polar region and run northwards, reentering the Earth at a location in Northern Canada. Open field lines are those nearer to the poles that do not reenter the Earth, but extend outward to combine with the Sun's Interplanetary Magnetic Field (IMF). The boundaries between open and closed field lines are known as the High Latitude Trapping Boundaries (HLTBs), and exist roughly at ± 65 -70 degrees from the magnetic equator².

Energetic particles of either interplanetary or atmospheric origins can become entangled along closed field lines due to the Lorentz force. If a particle has a non-zero velocity component parallel to the field line, it will gyrate along the line. However, as the particle approaches a pole, the field strength increases, diminishing the magnitude of the parallel component. Eventually, at locations called *mirror points*, this parallel component will go to zero, stopping the particle's forward motion³.

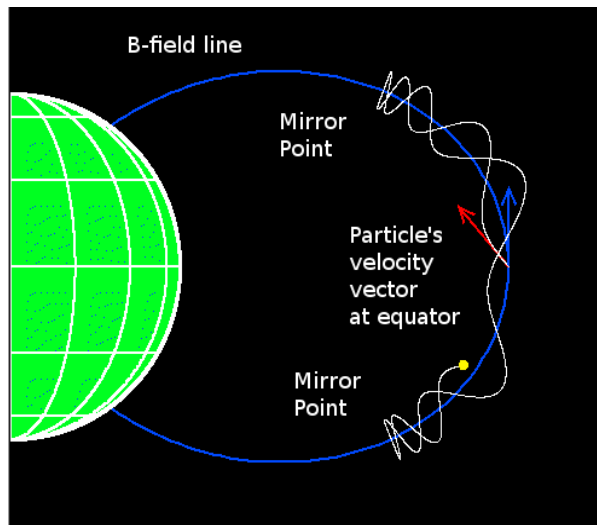


Figure (1) Schematic drawing showing the interaction of a charged particle (yellow) and a magnetic field line (blue). The pitch angle at the equator (shown in red) determines the location of the mirror points. (Figure adapted from <http://www.altfuels.org/sampex/losscone/index.html>)

If a mirroring point occurs at sufficient altitude, usually above 100 km, the particle will reverse direction, or “mirror back”, along the line toward the opposite pole. Such a particle is said to be trapped. Conversely, if the particle manages to reach a height less than 100 km, collisions with atmospheric neutrals are likely to occur and the particle may be lost to the atmosphere. The locations of mirror points are determined by pitch angles (defined as the angle the particle's velocity vector makes with the field line) at the magnetic equator. As such, particles with large equatorial pitch angles (i.e. small parallel velocity components) will mirror *before* particles with small equatorial pitch angles (i.e. large parallel velocity components) and are more likely to be lost. The set of pitch angles that will likely result in lost particles is called the *loss cone*³. (See Figure (2)).

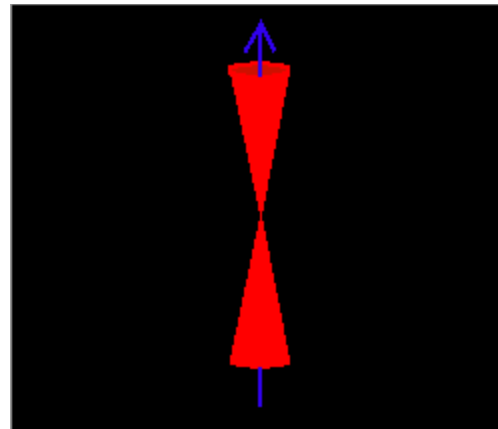


Figure (2) Loss cone. Any particles with equatorial pitch angles that lie inside the loss cone will not be mirrored back along the field line; they are not trapped (Figure from <http://www.altfuels.org/sampex/losscone/index.html>)

Mapping of the HLTB

Previous satellite missions have shown that the HLTB migrates as a result of ionospheric phenomena and spaceweather conditions. Nevertheless, a complete mapping of the HLTB has yet to be accomplished. To address this problem, students at Boston University are currently constructing two satellites, collectively known as the TIME CubeSats, that will perform a more thorough reconnaissance. Placed in polar orbits, both satellites will allow us to image the HLTB eight times per orbit (four observations per satellite, two in the northern hemisphere and two in the southern hemisphere). Their flight configuration will give us accurate temporal and spatial data regarding the boundaries' dynamics and their response to external forcing. Furthermore, the TIME mission will shed light on other mechanisms by which particles become scattered and lost to the atmosphere.

In this paper we report on the development of the powerful sensor system which will be integrated into the TIME CubeSats. Called the Compact Half-unit Imaging electron spectrometer for CubeSat Operations (CHICO), this novel device not only bears a close similarity to the the Fixed Sensor Head (FSH) instrument soon to be flown on the Air Force DSX mission⁴, but will provide CubeSat designers with a low-cost and compact, yet versatile, tool for near-Earth space exploration.

SYSTEM OVERVIEW

Based on the Loss Cone Imager (LCI or Fixed Sensor Head, FSH) instrument from the DSX mission, CHICO aims to provide a compact Imaging Electron Spectrometer (IES) and supporting electronics for spaceweather research.

Like the FSH, CHICO's IES incorporates silicon detectors to measure particle flux as a function of latitude. Amplification and shaping of acquired signals is accomplished with a Readout Electronics for Nuclear Applications (RENA³) chip, an ASIC originally developed for medical tomography applications.

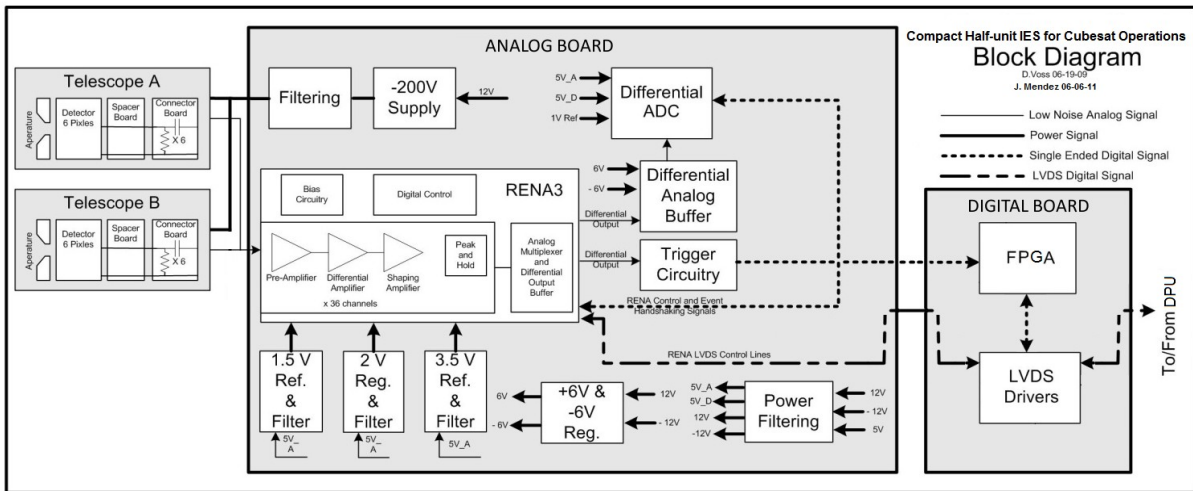


Figure (3) Overall block diagram of the CHICO instrument

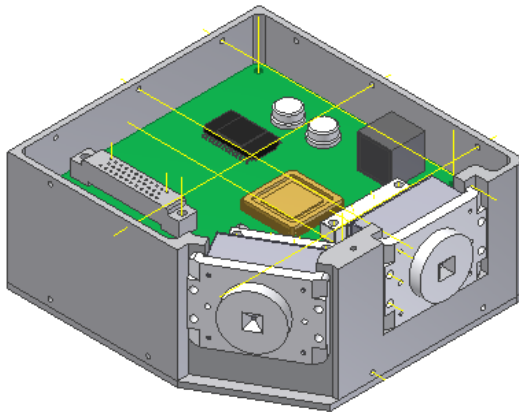


Figure (4) Autodesk CAD model of the enclosed Analog and Digital Boards. The top lid has been removed to show the Analog Board populated with the RENA, the ADC and detector mounts.

The IES is comprised of two main parts: the Analog Board and the Digital Board. The analog board houses the RENA chip, an ADC and detector connectors, while the digital board contains the Xilinx FPGA.

In broad terms, CHICO operates as follows: When a particle collides with a detector, a small amount of charge appears at one of the 36 RENA inputs. Internal RENA circuitry amplifies and shapes this signal into an analog voltage proportional to the particle's energy. An external ADC digitizes the processed information. Parallel digital data is then read by the FPGA and formatted into packets. Packets can then be transmitted over LVDS lines to the satellites' Data Processing Units (DPU) where they are stored or prepared for ground transmission.

CHICO, however, does differ significantly from the FSH in a number of ways. As mentioned previously, the size of the IES has been shrunk drastically, permitting CHICO to be integrated on CubeSat missions. This reduction only allowed us to include two six-pixel detector telescopes into the CHICO design (the FSH had three-telescope detectors). One telescope points

along the satellite axis direction, while the second one points 60 degrees away from this axis. Additionally, while the analog and digital portions of the FSH IES were housed in separate structures, CHICO's Analog and Digital Boards fit within a single aluminum housing. Finally, to reduce the cost of the system, non-radiation-hardened parts were employed in the system design (It should be noted, however, that RAD-hard parts can be easily integrated into the current system).

TELESCOPE DETECTORS

CHICO makes use of a pair of Si solid state detectors (SSD) to measure energetic particles. Comprised of 6 pixels each, the SSDs have the capacity to measure particle energies in the range of 30 keV to 500 keV⁴ along with the associated pitch angles (See Figure (3)). Given that each detector has a 10 ° by 10 ° field of view, the CHICO instrument is able to image a 120 ° by 10 ° region of the sky.

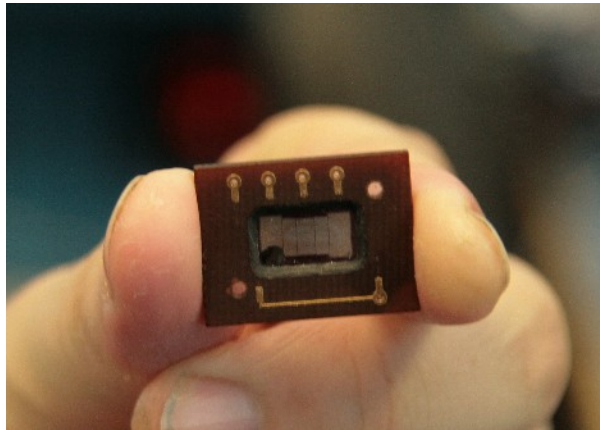


Figure (5) Photograph of one of the six-pixel detectors

The detectors are approximately 1000 ±50 microns thick. CHICO's telescope design (which is same as the FSH design) uses a pinhole configuration, enabling the device to operate in high-particle flux regions such as the radiation belts.

As shown in Figure (6), a detector can be modeled as reverse biased *p-n* diode junction. When a particle impacts a pixel, an electron-hole pair is created. A large reverse biasing potential applied to the p-type contact (-200 V in the present case) drastically expands the depletion region along the *p-n* junction, ensuring that any produced charge carriers are rapidly swept to the detector contacts. The electron-hole production is described by Equation (1),

$$Q = W/\epsilon \quad (1)$$

where Q = number of electron-hole pairs produced per incident particle, W = the energy lost in the ionizing material and ϵ = the radiation-ionizing energy⁴.

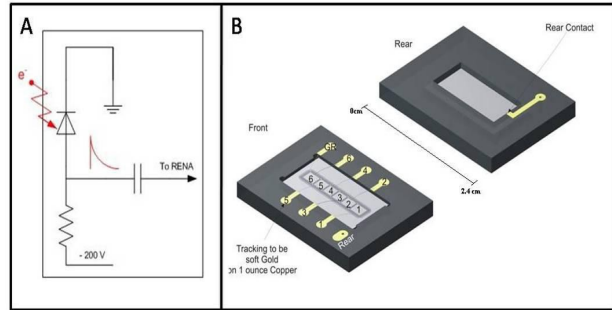


Figure (6) a. Diode model of a Si detector b. Schematic of the IES detectors

One of the advantageous properties of Si is that ϵ has only a weak dependence on the type of incident radiation. As such, the number of created electron-hole pairs, Q , is primarily a function of the energy lost to the ionizing material when a collision occurs. It is this linear relationship that makes silicon detectors well-suited candidates for spaceweather research. For a more detailed description of the physics behind Si detectors, the reader is referred to Klien (1968)⁵.

SYSTEM DESIGN: ELECTRICAL

The Readout Electronics for Nuclear Applications

The heart of the CHICO instrument is the Readout Electronics for Nuclear Applications (RENA³), a pulse amplification and shaping application-specific integrated circuit (ASIC) originally designed for medical applications⁶. Recently, however, the RENA has been considered for space-based missions. With 36 analog inputs, the RENA represents a powerful tool to explore the interaction between high-energy particles and the magnetosphere⁴.

When an particle impacts one of the detector pixels, a small amount of charge (9 fC to 54 fC) is deposited on the corresponding RENA input pin⁶. The first stage within a RENA channel is a low noise preamplifier. A feedback capacitor can be set to 15 or 60 fF and the feedback resistor can be configured to 200 M-ohm or 1.2 G-ohms. Given that this feedback loop will determine discharge time for the pre-amp, the user must adjust the capacitor and resistor values depending on the expected particle count rate. Other settings for the pre-amp include pole-zero cancellation and input pulse polarity³.

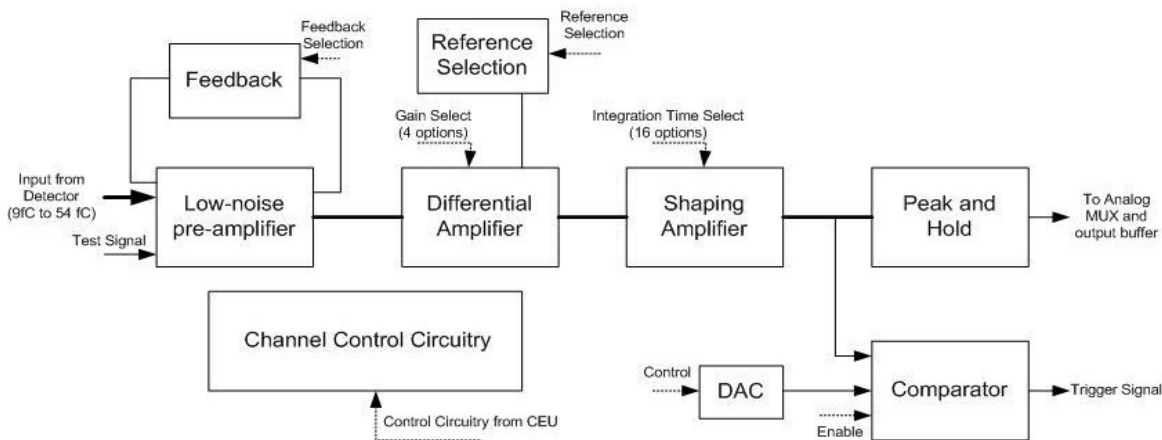


Figure (7) Block diagram of a single RENA Channel (Adapted from Voss, 2008)

The next stage in a channel is a differential amplifier AC coupled to the pre-amp through a blocking capacitor. External reference voltages must be provided by the user. Selection of these voltages depends on the expected polarity of incoming signals. In the present case, external reference voltages of 3.5 and 1.5 V are employed.

The RENA alerts the FPGA when an event has occurred. The FPGA proceeds, through a complex handshaking routine, to multiplex the amplified analog data to a differential output. At this point, the data is buffered and passed to a 12-bit pipe-lined analog-to-digital converter. Data is then received by the FPGA, where it is formatted into packets ready for transmission to ground or on-board storage₃.

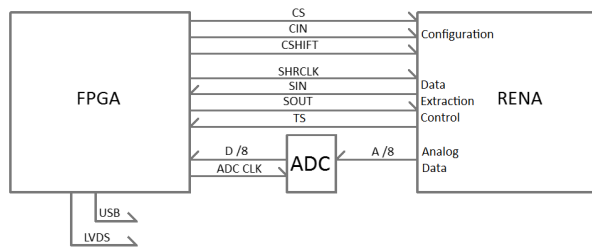


Figure (8) RENA-FPGA interface

After the differential amplifier, signals are processed by a shaping amplifier with 16 user-selectable integration times. Once shaped, a signal is passed to a peak-and-hold circuit. The event-level threshold is set by an 8-bit digital to analog converter. Both the outputs of the the shaping amplifier and the DAC are fed to a comparator. When the signal in the peak-and-hold exceeds the threshold level, the shaped value is multiplexed to the RENA's differential analog output buffer. A block diagram of a single RENA channel is shown in Figure (7).

RENA Configuration and testing

Upon power-up, the FPGA configures the RENA by shifting a 41-bit word into a shift-register within the ASIC. Configuration is accomplished with the use of three signals – Configuration Select (CS), Configuration Shift (CShift) and Configuration Input (Cin). The 41-bit is shifted into the RENA by sending a clock signal to the Cshift pin, while passing configuration bits to the Cin pin. Once the entire word has been passed to the RENA, the CS pin is pulsed to lock that configuration into the RENA's registers.

Each channel on the RENA is independently configurable. Gains, input pulse polarity and integration time are set by a word sent from the instrument control unit, in our case a Xilinx FPGA on the Digital Board.

Testing and calibration of a channel can be done by means of an external circuit which provides a known energy deposition to a channel input via a specialized test pin. Individual channels can be connected to this test pin by setting the appropriate bit in the RENA configuration word. The circuit is composed of an NPN bi-polar junction transistor, whose base is connected to a digital I/O on the FPGA. When pulsed by the FPGA, the transistor will allow current to flow through a voltage divider. The test pin is wired to the output of the divider and a generated test pulse will charge a 75fF coupling capacitor within the RENA. The collected charge is then deposited on the input of all RENA channels that have been selected for calibration in the

configuration word. The capacitor provides a charge injection of 75fC/V on each ramp of the test pulse. A pad for a variable resistor is included parallel with the lower resistor of the voltage divider. This allows the user to appropriately scale the height of the test pulse. The pulse width should be longer than the selected shaping time to ensure that all of the charge of a pulse edge is seen by the peak detectors.

A second testing method involves simulating a particle hit with a dedicated pulser unit such as a 448 Ortec. The Analog Board contains a male SMA connector wired to one of the 36 inputs for this purpose.

Supporting Electronics

Once a signal or event has been shaped and amplified, an analog voltage will appear at the RENA's differential output. This output, comprised by voltages AOUT+ and AOUT-, is centered at 2.5 V. The largest signal occurs when AOUT+ is 3V and AOUT- is 2V. Conversely, 3V at AOUT- and 2V at AOUT+ is representative of the smallest values. Due to the small driving capacity of the differential output, AOUT+ and AOUT- are buffered using a pair of high-speed, precision operation amplifiers configured in voltage follower mode (unity gain).

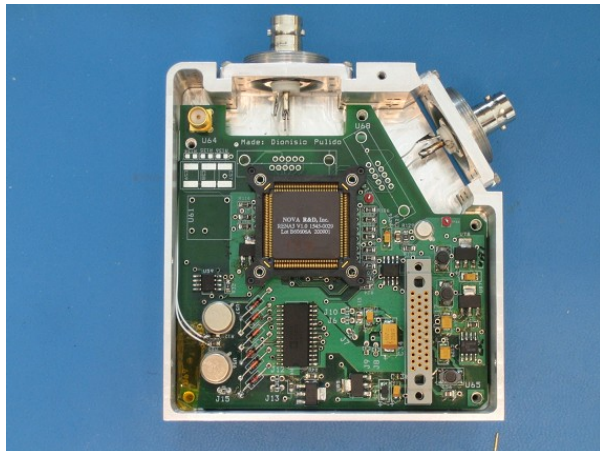


Figure (9) CHICO Analog Board

Our design allows digital conversion to be performed by either an Analog Devices AD9225 or a Honeywell HMXADC9225 12-bit, pipe-lined analog-to-digital converters configured to operate in differential mode. Only the 8 most significant bits are used.

Digital Design

We employ a Xilinx Spartan-3 XC3S50AN FPGA for RENA control, data extraction and packetizing. The Spartan-3s are a low-cost, albeit powerful line of non-volatile FPGAs. The XC3S50AN is available in a thin quad flat pack (TQFP) package. CHICO can either transmit data serially via a USB FTDI chip (used for testing and calibration) or LVDS, which provides excellent noise immunity. Future modifications will include the ability to transmit data using Bluetooth technology.

SYSTEM DESIGN: MECHANICAL

Both the Analog and Digital Boards are housed within one half of a standard CubeSat unit (10x10x5 cm). The housing is made of 6061 aluminum (Figure (10)). To reduce noise, the Analog Board is separated from the Digital Board by a metallic plane within the housing. A rectangular hole in the plane allows a stackable connector to pass signals between the two boards. Thermal planes on both the Analog and Digital boards are connected to the board mount holes, permitting excess heat from the electronics to be dissipated in the mechanical structure. Lids on either side provide complete instrument enclosure.

A 21-pin microD connector brings LVDS signals out of the instrument enclosure. This connector follows the pin-out defined by the Boston University Student-Satellite for Applications and Training (BUSAT) intra-satellite communication standard defined during the Nanosat 5 competition.

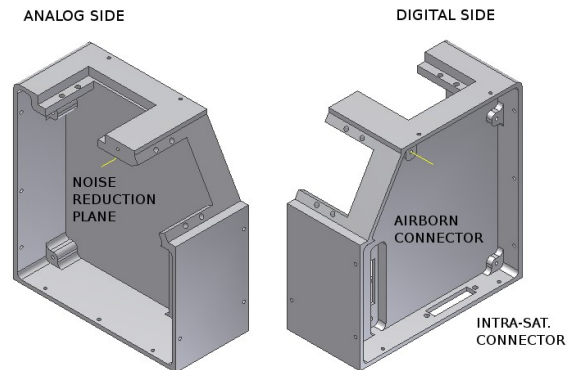


Figure (10) Instrument mechanical enclosure

The instrument can be mounted to the CubeSat structure either with Wedge-Lok technology or 2-56 size screws.

INSTRUMENT PERFORMANCE and GENERAL CHARACTERISTICS

Extensive testing was performed on the FSH, CHICO's direct precursor, during the development of the LCI instrument³. Depending on pre-amplifier gain selection for the RENA, energies between 20 and 880 keV can be measured (our Si detectors do not allow this range, however). The default gain for the FSH and CHICO RENA is 2.3, permitting particles with energies of 30-500 keV to be characterized. Because of imperfections in the chip manufacturing process, small variations in performance exist between individual channels and individual RENA chips. This means that the behavior of each channel must be determined independently.

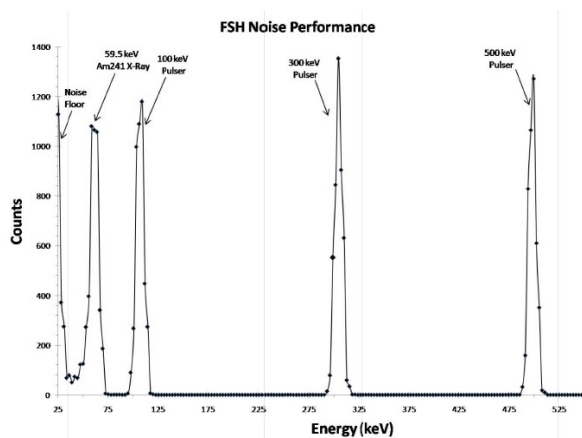


Figure (11) FSH noise performance using an Americium-241 X-ray source and a research pulser. RENA pre-amp gain = 2.3 (From Voss, 2009)

Voss et al (2009) have tested the RENA and detectors in their FSH instrument using pulser units, an array of radioactive sources and particle accelerators. To characterize noise performance, they determined the Full Width Half Maximum (FWHM) of the system. This was done by exposing the instrument's telescopes to particles whose energy values spanned the valid measurement range (30-500 keV). Figure (11) exemplifies the response of the FSH to both an Americium-241 X-ray source and a pulser mimicking particles with energies of 100, 300 and 500 keV⁴. The noise floor can be seen to the far left.

At the time this manuscript was written, preliminary tests were conducted on the CHICO instrument. The close resemblance CHICO has to its forebearer makes us confident that our instrument will perform similarly to the FSH. Extensive testing and further instrument evaluation will be conducted during the summer of 2011.

Table (1) is a summary of CHICO's specifications

Mass	0.3 kg
Volume	< 0.5 Unit
Power	<2 W (12V,-12V and 5V)
Data rate	15 kb/s
Instrument FOV	120 degrees
Energy spectrum	30 keV – 500 keV

Table (1) Instrument Specifications

A FIRST MISSION

As mentioned in the introduction of this paper, two satellites are currently being developed at Boston University along with CHICO. Named the Twin Imaging of the Moving Electron trapping boundary (TIME) CubeSats, these 1.5 Unit satellites will serve as the test vehicles for the CHICO system. They are designed to launch concurrently from a single PPOD and then separate. TIME will offer a cost-effective platform for studying the high-latitude trapping boundary and other magnetospheric phenomena. Figure (12) depicts CHICO integrated into one of the TIME structures.

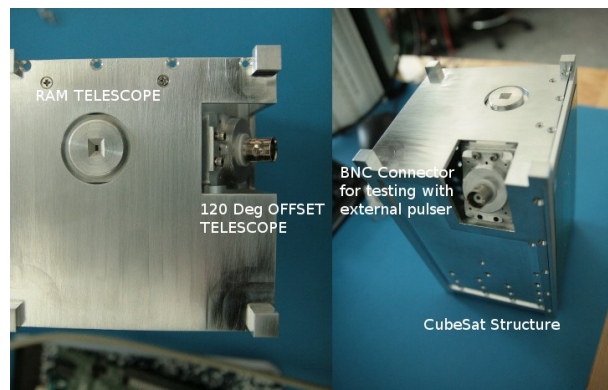


Figure (12) CHICO integrated into one of the TIME CubeSats

In addition to the IES, each CubeSats will fly small, three-axis magnetometer that will provide measurements of the local B-vector in satellites' coordinates. The data from both CHICO and the magnetometer will grant us the means to accurately determine electron pitch-angles. Furthermore, the combined efforts of two CubeSats will enable the separation of spatial and temporal effects. Such effects detrimental and are unobtainable on single spacecraft studies.

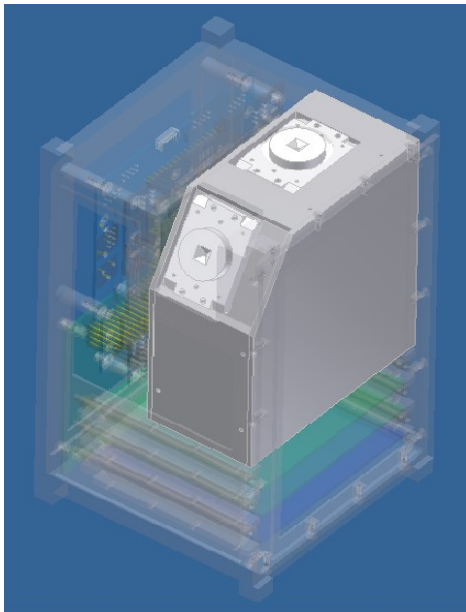


Figure (13) CAD model of one of the TIME CubeSats, including CHICO and a ClydeSpace EPS

The main science goals of the TIME mission regarding the HLTB can be condensed as follows:

- Develop a better understanding of the motion of the radiation belt trapping boundary and its relation to space weather activities.
- Identify how scattering modifies the pitch angles of energetic particles within the trapping boundary, and identify the roles different scattering and/or acceleration mechanisms are playing.

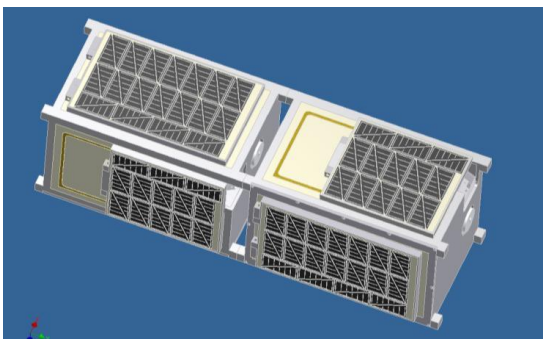


Figure (14) TIME CubeSats as will be placed in a PPOD launcher

It is worth noting that the TIME CubeSat Mission is a completely student-driven interdisciplinary project which has involved people from the Electrical and Mechanical Departments in the College of Engineering, as well as members of BU's Physics Department. Moreover, we have begun to collaborate with students at the Universidad Interamericana campus Bayamon in Bayamon, Puerto Rico.

Efforts to bring the TIME mission forward will continue throughout the fall of 2011 and spring of 2012. TIME will undoubtedly encompass several senior design projects and senior theses.

CONCLUSION

We have developed a small, yet power imaging electron spectrometer called CHICO based on the Fixed Sensor Head instrument soon to be flown on the DSX satellite. The key features of CHICO can be summarized by the following points:

- CHICO's minute volume—less than that of half a standard CubeSat Unit—makes the instrument particularly suited for small, low-cost missions like the student-build TIME satellites. Similarly, it's small size and configuration make it amenable to modular satellite buses like the BUSAT.
- Expected performance similar to that of the FSH instrument, with an ability to detect particles with energies between 30keV and 500 keV.
- CHICO will provide an innovative and cost-effective platform to thoroughly explore the High-Latitude Trapping Boundary regions of the radiation belts

ACKNOWLEDGMENTS

The authors of this paper would like to thank the following individuals for their support during the development of the project:

Masato Nakanishi, Micheal Lloyd, Orin Hall, Xiang He Nate Darling, and Robert Kingsland.

REFERENCES

- [1] Turcotte, D. L and G. Schubert (2002) Chapter 1: "Plate Tectonics" Geodynamics, 2nd Edition, Cambridge Press

- ² Fritz, T. A. High-Latitude Outer-Zone Boundary Region for 40-keV Electrons during Geomagnetically Quiet Periods. *Journal of Geophysical Research, Space Physics*. Vol. 73, NO. 23, December 1, 1968
- ³ Spjeldvik, W. N. and P. L. Rothwell (1985) Chapter 5: “The Radiation Belts” *Handbook of Geophysics and the Space Environment*, pp 5.1-5.10.
- ⁴ Voss, D., A. Gunda, D. Carssow, T.A. Fritz, A. Mavretic and J. Sullivan (2009). Overview of the Loss Cone Imager Fixed Sensor Head Instrument. *Proceedings of SPIE*, doi: 10.1117/12.827366
- ⁵ Klein, C. (1968). Bandgap Dependence and Related Features of Radiation Ionization Energies in Semiconductors. *Journal of Applied Physics*, 19 (4), 2029-2038.
- ⁶ Tumer, T., Cajipe, V., Clajus, M., Hayakawa, S., & Volkovskii, A. (2006). Multi-Channel Front-End Readout IC for Position Sensitive Solid-State Detectors. *IEEE Nuclear Science Symposium* (pp. N14-19). San Diego : IEEE.
- ⁷ Spanjers, G., J. Winter, D. Cohen, A. Adler, J. Guarnieri, M. Tolliver, G. Ginet, B. Dichter, and J. Summers (2006) “The AFRL Demonstration and Science Experiment (DSX) for DOD Space Capability in the MEO” *Proceedings of the IEEE Aerospace Conference*, no. 1616

Images 1 and 2: Mark Looper (2000) Mark Looper's SAMPEX Data Page [Online] Available at: <http://www.altfuels.org/sampex/losscone/index.html> [Accessed 2011]